Applied Artificial Intelligence
An International Journal

ISSN: 0883-9514 (Print) 1087-6545 (Online) Journal homepage: https://www.tandfonline.com/loi/uaai20

High Frequency Transformer Design and Optimization using Bio-inspired Algorithms

Jeyapradha Ravichandran Banumathy & Rajini Veeraraghavalu

To cite this article: Jeyapradha Ravichandran Banumathy & Rajini Veeraraghavalu (2018) High Frequency Transformer Design and Optimization using Bio-inspired Algorithms, Applied Artificial Intelligence, 32:7-8, 707-726, DOI: 10.1080/08839514.2018.1506969

To link to this article: https://doi.org/10.1080/08839514.2018.1506969

APPLIED ARTIFICIAL INTELLIGENCE
2018, VOL. 32, NOS. 7–8, 707–726
https://doi.org/10.1080/08839514.2018.1506969

High Frequency Transformer Design and Optimization using Bio-inspired Algorithms

Jeyapradha Ravichandran Banumathy and Rajini Veeraraghavalu

Department of Electrical and Electronics Engineering, Sri Sivasubramaniya Nadar College of Engineering, Kalavakkam, Tamilnadu, India

ABSTRACT
High frequency (HF) transformer at the isolation stage of SST plays a vital role in deciding the power conversion efficiency of the SST system. This paper proposes a new design procedure for optimization of HF transformer used in SST applications such that it fulfils all the requirements pertaining to its operating conditions. The novel design procedure proposed is based on optimizing the core geometry (in 5th power of cm), which has direct influence on regulation and copper loss. An isolated half-bridge DC–DC converter topology is chosen for implementing the proposed design. Four bio-inspired algorithms, namely Particle swarm optimization (PSO), Whale Optimization algorithm (WOA), Dragonfly Algorithm (DA), and Ant Lion Optimizer (ALO) are used to solve the optimization problem and the results are compared with Genetic algorithm (GA). Finally, the optimization results are validated through PowerEsim, a web-based testing platform with huge database of real-time components from leading manufacturers across the globe.

Introduction

The evolution of Solid State Transformer (SST) in recent years as a promising new class of grid assets can be attributed to their ability to offer service extensions beyond voltage transformation, such as provision for dual power output (both dc and ac), input–output decoupling, high switching frequency, fault isolation, better power quality, etc. The heart of the SST system is the high frequency (HF) isolated dc–dc converter, which provides galvanic isolation between the medium voltage AC grid and a low voltage AC/DC grid as shown in Figure 1. Though the choice of HF results in reduced footprint for the transformer, it also leads to higher switching losses and saturation of magnetic components. Further, the reduction in footprint entails an increased loss density in the transformer, which necessitates significant efforts on thermal management (Meier et al. 2009). Thus a robust design procedure is required which collectively addresses the HF, isolation and

CONTACT Jeyapradha Ravichandran Banumathy jeyapradharb@ssn.edu.in Department of Electrical and Electronics Engineering, Sri Sivasubramaniya Nadar College of Engineering, Rajiv Gandhi Salai, Kalavakkam, Tamilnadu, India, 603110.

Color versions of one or more of the figures in the article can be found online at www.tandfonline.com/uaai.

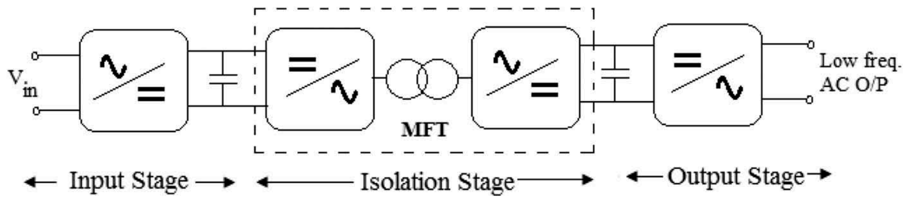

Figure 1. Basic three stage SST architecture.

thermal management issues and yields desired efficiency concurrently retaining the %regulation and power losses within specified limits.

Numerous high/medium frequency transformer design solutions for various applications were established in literature. Earlier, researchers have attempted to develop detailed HF transformer design for switching power supplies (Coonrod 1986; McLyman Colonel 1993; Pressman 1998; Rama Rao et al. 2004). The design considerations of medium frequency transformers for railway traction applications were discussed in literature in the previous decade (Kjellqvist, Norrga, and Ostlund 2004; Steiner and Reinold 2007). The design optimization of high/medium frequency transformers for DC offshore applications was also documented in the past (Bahmani 2014; Bahmani, Thiringer, and Kharezy 2015). Research efforts on design of high/medium frequency transformers for SST applications have been widely reported in literature (Du et al. 2010; Huina, Xiaodong, and Gang 2012; Ortiz et al. 2013; She et al. 2014; Montoya, Mallela, and Balda 2015).

Further, a thorough survey of literature reveals that research contribution toward HF transformer design have come in the way of optimizing the core based on area product (Farhangi and Akmal 1999; McLyman 1993), optimizing the flux density of the core and current density of the windings (Petkov 1996), optimization including HF effects (Hurley, Wolfle, and Breslin 1998), optimization with arbitrary current and voltage waveforms (Breslin, 2002), high isolation requirements and thermal management (Ortiz, Biela, and Kolar 2010), minimizing the losses taking leakage inductance and phase shifted angle of the converter into consideration (Hoang and Wang 2012), optimization with emphasis on thermal and insulation design (Peng and Jurgen 2013) and maximizing the power density by accounting for tuned leakage inductance (Bahmani M.A. 2014; Bahmani M.A. et al. 2015).

All the aforementioned research efforts focus on either single or multi-objective optimization with or without single/multiple constraints with a procedure involving verification of bounds for parameter values other than constraints before arriving at an optimal solution to the problem. This is a time-consuming process as every time an operating parameter is found to infringe the bounds, the optimization algorithm searches for another optimal solution satisfying the bounds.

This paper is intended to present a simple, yet robust optimization procedure for the design of HF transformer based on core geometry coefficient (defined by McLyman 1993) with a constraint imposed on its specific loss. The proposed procedure circumvents the verification of parametric limits for producing an optimal solution as the optimal core geometry (in 5th power of cm) directly brings all the operating parameters like %regulation and temperature rise within preferred limits without compromising on efficiency. Moreover, the proposed procedure is less time consuming than the methods documented in literature as it does not involve verification loops for bounds on operating parameters. Above all, in contrast to other methods where attention need to be paid to avoid saturation effects on magnetic components, the proposed optimization does not have this issue as the core selection is made only after obtaining the optimal core geometry.

The proposed optimization is executed on an isolated half-bridge dc–dc converter with few of the latest bio-inspired algorithms, which are proved to be highly efficient compared with GA. The results of optimization are validated through PowerEsim which unlike other simulation tools is built with practical power supply modules and components from leading manufacturers in the market (Poon 2009).

Isolated half bridge DC–DC converter

A number of dc–dc converter topologies for SST applications have been investigated in the past (Kolar and Ortiz 2014; Shri 2013) and their relative merits and demerits discussed. Since the primary objective here is the design optimization of HF transformer, a simple half bridge dc–dc converter topology is chosen for unidirectional and Modular SST applications. However, the design optimization can be carried out with any dc–dc converter topology that is deemed appropriate for a particular application.

Figure 2 shows the basic converter schematic and the associated waveforms of a half-bridge isolated dc–dc converter. The element for energy transfer is the leakage inductance of the transformer. The switches S_1 and S_2 are turned on with a phase shift of 180° and both experience a voltage stress equal to that of the input voltage, in contrast to twice the input voltage as in push–pull and forward converters (Vinnikov, Jalakas, and Egorov 2008). Also, the magnetization of the isolation transformer is bidirectional and hence there is no need for a demagnetizing circuit. Other advantages of this converter include less primary turns for the same input voltage and power, lesser winding costs, lower proximity effect losses, no danger of transformer saturation, reduced cost, and its ability to be scaled up to higher power levels.

The apparent power of the transformer in a half bridge converter is calculated as follows:

Secondary apparent power for tapped winding,

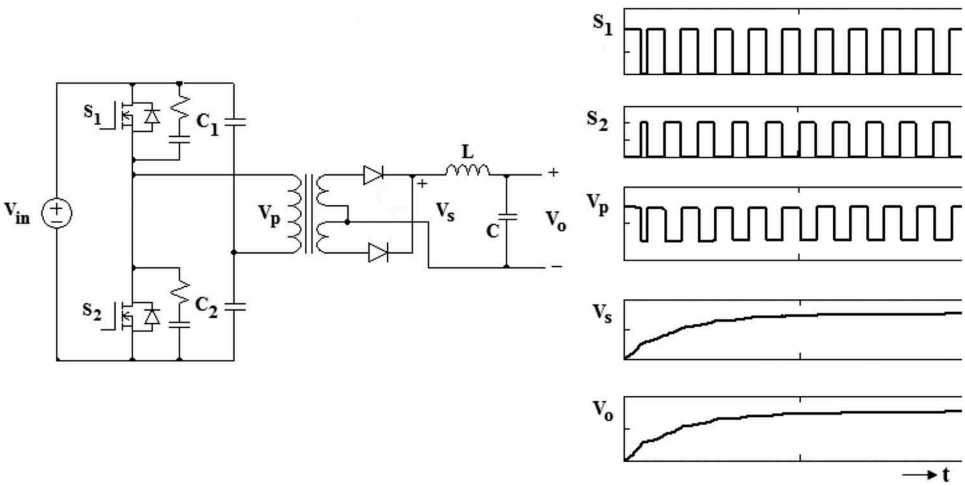

Figure 2. Schematic of isolated half-bridge converter and its associated waveforms.

$$P_{sy} = (V_o + V_d)I_o * \sqrt{2} \tag{1}$$

where V_o and I_o are output voltage and current respectively and V_d is the diode voltage drop.

Primary apparent power,

$$P_{py} = \frac{P_{sy}}{\eta} \tag{2}$$

Thus, total apparent power

$$P_t = P_{py} + P_{sy}\,\text{Watts} \tag{3}$$

The d.c. transfer function of the half bridge converter is derived as

$$\frac{I_{in}}{I_o} = \frac{V_o}{V_{in}} \approx \frac{1}{2} \cdot \frac{N_s}{N_p} \cdot \frac{2t_{on}}{T} \tag{4}$$

Design optimization

Procedure

While most of the proposed design methodologies for HF transformers were based on a specified temperature rise, they can also be designed for a given % regulation, "α". As per definition by (McLyman 1993), α is associated with two coefficients namely, the electrical coefficient "K_e" and the core geometry coefficient "K_g" given by

$$K_e = 0.145\left(K_f\right)^2 f^2 {B_m}^2 \times 10^{-4} \tag{5}$$

$$K_g = \frac{P_t}{2K_e\alpha} \tag{6}$$

where K_f is the waveform coefficient, P_t is the total apparent power in Watts, f is the operating frequency in Hz, and B_m is the flux density in tesla.

Alternately, K_g can be expressed as

$$K_g = \frac{W_a {A_c}^2 K_u}{MLT}\ \text{cm}^5 \tag{7}$$

where W_a is the window area in cm^2, A_c is the effective core cross-section in cm^2, K_u is the window utilization factor, and MLT is the mean length of the turn in cm.

From Equations (6) and (7), it is noted that K_g not only influences the size of the magnetic components but also affects the regulation and copper loss. Thus by optimizing K_g, it is possible to design a transformer, which is more compact and efficient, simultaneously holding the other key design requirements like %regulation, current density in the windings, copper losses, temperature rise etc., within specified bounds.

Referring to Equations (5) and (6), it is clear that K_g is a function of two variables namely, f and B_m with fixed %regulation. Though flux density in the core is actually a function of operating frequency, a good trade-off is needed between these two parameters such that optimum core geometry is achieved. Therefore, while optimizing K_g, frequency and flux density are chosen as the free parameters. The variation of core geometry coefficient with operating frequency and flux density is depicted in Figure 3.

The optimization problem in general is stated mathematically as follows:

Find $X = [X(1)\ X(2)\ldots X(n)]$, such that $F = f(X)$ is minimum subject to

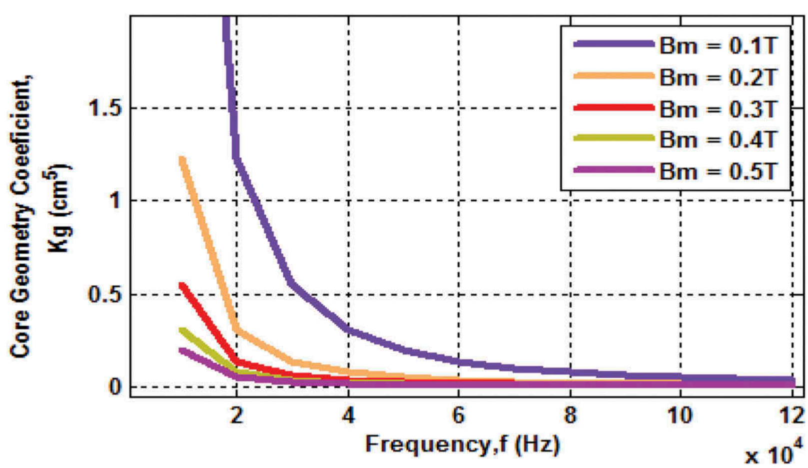

Figure 3. Plot of core geometry coefficient with frequency.

$X_{imin} < X(i) < X_{imax}$ where $i = 1,2\ldots n$ and $C_i\ (X) < 0,\ i = 1,2,\ldots m,$

where $X(1), X(2),\ldots\ldots X(n)$ represent the set of independent design variables with X_{imin} and X_{imax} as their lower and upper bounds respectively. $F = f(X)$ is the objective function to be optimized and $C_i(X)$ are the design constraints.

Minimize K_g such that
(i) $f_{min} < f < f_{max}$
(ii) $B_{mmin} < B_m < f_{mmax}$

with the constraint $W_{pk}\ (f,B_m) - 0.05{*}P_t < 0^{\dagger}$
where W_{pk} is the specific loss in W/Kg and P_t is the total apparent power in watts.
† Specific loss is assumed to be limited to 5% of total apparent power.

With f and B_m chosen as two independent design variables and K_g as the objective function to be minimized with a constraint imposed on the specific loss of the transformer, the design problem can now be stated as follows.

The design flowchart for the proposed optimization procedure is depicted in Figure 4. The design equations are presented in the Appendix. The inputs to the design problem are power output and voltage levels of the converter. Efficiency and regulation in percentage, waveform coefficient and window utilization factor are chosen to be the fixed parameters. Contrary to the design of low frequency transformer where V/f is held constant to avoid over-fluxing, the operating frequency here is swept across specified limits along with maximum flux density as the choice of core and its dimensions are made only after establishing the optimum core geometry.

Once the best values for the free parameters are found and the optimal value for core geometry coefficient is established using latest bio-inspired algorithms, suitable core material is selected from the core data table corresponding to the optimal value. If there is no precise match for the optimal core geometry coefficient from the core data table, then the core with next higher value for K_g is chosen to ensure minimal copper loss.

The dimensions of the selected core and their specifications are extracted from the table. With these dimensions and specifications, the current density in the windings, number of turns in the primary and secondary are calculated. The primary and secondary wire areas are then calculated and a wire size with the required wire area is found from the wire table. Subsequently, primary and secondary winding resistances and hence copper losses are calculated. The new values for %regulation and flux density are then updated. The core losses and hence the total losses are calculated followed by the power density and temperature rise.

The design specifications of a single converter module are considered for evaluating the test cases presented in Table 1 of this paper. Several such modules

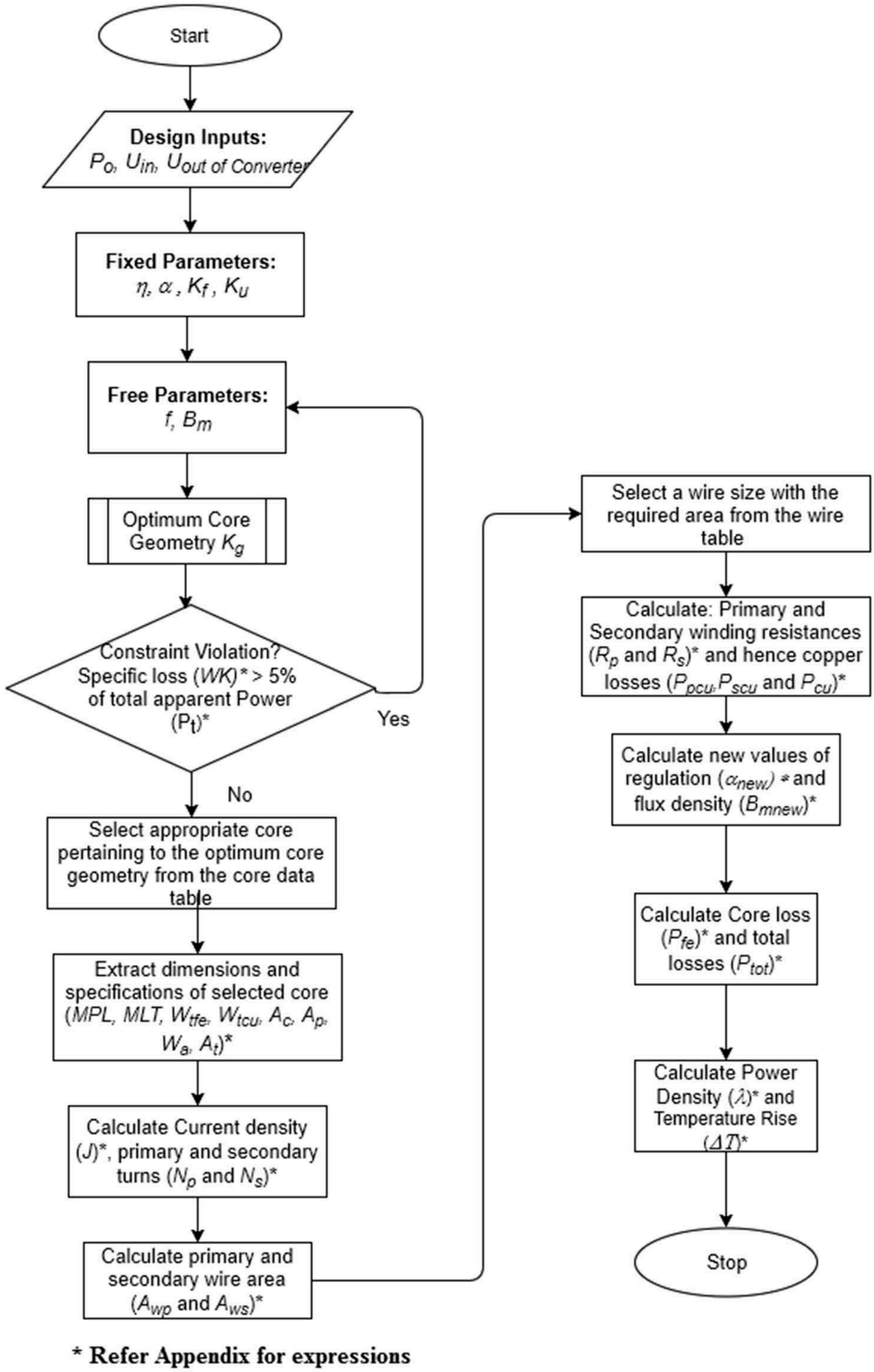

Figure 4. Flowchart for the proposed design optimization of high frequency transformer.

can be connected in parallel at the low voltage side (LVDC link) and in series at the high/medium voltage side (HVDC/MVDC link) as per requirement.

Algorithms for optimization

Nature-inspired optimization algorithms are being extensively applied nowadays to solve real and complex engineering design problems (Yang 2010). Earlier, GA has been widely applied to solve transformer design optimization problems (Coonrod 1986; Rama Rao et al. 2004; Yadav et al. 2011; Versèle, Deblecker, and Lobry 2012). However, more recently Artificial Bee Colony (ABC) and PSO algorithms have been employed to solve these problems (Davood, Mehdi, and Jawad 2016).

In this paper, Particle Swarm Optimization (PSO) algorithm along with three other recently developed algorithms namely, Ant Lion Optimizer (ALO), Dragon Fly Algorithm (DA), and Whale Optimization Algorithm (WOA) are applied to solve the proposed optimization problem and the results are compared with the conventional GA. The proposed optimization procedure is more simple and straight forward than the methods presented in the literature cited above.

The Ant Lion optimizer

This algorithm emulates the natural hunting behavior of antlions by modeling the interactions between antlions and ants in the trap (Mirjalili 2015). The stages involved in hunting process viz., random walk of ants, building traps, entrapment of ants in traps, catching preys, and re-building traps are modeled mathematically. The pseudocode for the algorithm along with a detailed analysis is presented in the reference cited above.

Dragon fly algorithm

This algorithm is inspired by the static (hunting) and dynamic (migration) swarming behavior of dragon flies in nature (Mirjalili, S. 2016b). The collective interaction of dragonflies in traversing, hunting for prey, and evading enemies are modeled as two vital stages of optimization: exploration and exploitation. Random values within specified bounds of variables are used to initialize the position and step vectors of dragon flies which are then updated iteratively until the required criterion is met.

Whale optimization algorithm

The social hunting behavior of humpback whales is used to model this algorithm (Mirjalili, S. 2016a). The three steps involved in the hunting process by Whales namely, tracking the prey, encircling the prey, and the bubble-net feeding behavior are modeled mathematically in order to perform optimization.

Optimization results and discussion

Three test cases are evaluated in support of the proposed optimization procedure and the design specifications for the same are listed in Table 1. A single module isolated half-bridge dc–dc converter is chosen for validating the test cases. For modular SST applications, a number of such modules can be cascaded as per requirements. Since the output power of half-bridge converter is limited to 750 W, the test cases are chosen accordingly. However, with higher end dc-dc converters, the power levels can be extended beyond 1 kW. The fixed parameters assumed for all the case studies are common and are presented in Table 2.

The operating frequency, f and the maximum flux density, B_m which influence the core geometry coefficient (Equations (5) and (6)) are chosen as the free parameters. They are swept over a wide range within specified bounds to find the best optimal value for K_g. The limits for the operating frequency are set between 10 and 120 kHz and that for the maximum flux density between 0.1 and 0.6 T. The upper boundary for flux density is usually set by the saturation flux density of the core material with a safety margin of 10–20% to avoid operation close to saturation. For the case studies considered in this paper, ferrite core is chosen as they have lower core losses (above 20 kHz) and are available in a wide variety of geometric shapes. The maximum value for saturation flux density of ferrite core is 0.45 T. Therefore, the upper limit for B_m is fixed at 0.6T.

Upon optimization using PSO, ALO, DA, and WOA, the best values for free parameters and the optimal core geometry are established. A comparison of performance of all the algorithms with GA for the three test cases is presented in Table 3. All the four nature-inspired algorithms are compared

Table 1. Design specifications of a single converter module.

	Test cases		
Design parameters	I	II	III
Output power, P_o (W)	250	500	750
Nominal input voltage, V_{in} (V)	100	325	500
Output voltage, V_o (V)	48	100	200
Output current, I_o (A)	5.2	5	3.75

Table 2. Fixed parameters for optimization.

% Regulation, α	0.57
% Efficiency, η	96
Waveform coefficient, K_f (for square wave)	4.0
Window utilization factor, K_u	0.4

Table 3. Comparison of performance of optimization algorithms.

Test cases		Operating frequency, f_best (kHz)	Maximum flux density, B_{m_best} (T)	Core geometry coefficient, K_{g_opt} (cm^5)	Average overall computational time (s)	Average no. of iterations for convergence
I	**GA**	74.76	0.1000	0.04496	84.70	27
	PSO	74.76	0.1000	0.04496	1.46	231
	DA	74.76	0.1000	0.04496	64.72	278
	ALO	74.76	0.1000	0.04496	13.25	312
	WOA	74.76	0.1000	0.04496	5.12	19
II	**GA**	99.68	0.1088	0.041776	78.80	25
	PSO	99.99	0.1088	0.041539	1.24	229
	DA	99.99	0.1088	0.041539	52.24	280
	ALO	99.99	0.1088	0.041539	11.09	320
	WOA	100	0.1088	0.041539	4.66	20
III	**GA**	100	0.12571	0.046257	73.04	25
	PSO	100	0.12571	0.046257	1.15	212
	DA	100	0.12571	0.046257	60.31	272
	ALO	100	0.12571	0.046257	11.55	309
	WOA	100	0.12571	0.046257	4.84	23

on the basis of identical search agents (equal to 100). The computational speed and the number of iterations for convergence are averaged over 10 successive runs. For the case studies under consideration, it is discerned from the table that all the algorithms return identical optimal solution though they differ in computational speed and convergence. With less number of generations, the optimal value generated by GA is inconsistent in successive runs. However, with an initial population of 200 and increase in number of generations to 1000, GA produces a consistent solution at the cost of increased overall computational time.

The core data pertaining to the optimal value of K_g are listed in Table 4. For all the three test cases, the core having a K_g value slightly higher than the optimum K_g is selected. This is done to ensure minimal copper loss. The look

Table 4. Optimal core data.

Core data	Test Case I	Test Case II	Test Case III	Core data	Test Case I	Test Case II	Test Case III
Core material part no.	EE 43208	DS 43019	RM 42819	Min. core X-sectional area, A_c (cm^2)	1.299	0.96	0.98
Magnetic path length, MPL (cm)	4.17	4.62	4.4	Total window area, W_a (cm^2)	0.6048	0.7469	0.639
Total core weight, W_{tfe} (gm)	26	22	23	Area product, A_p (cm^4)	0.7802	0.717	0.6258
Total weight of copper, W_{tcu} (gm)	19.21	17.32	11.81	Overall surface area of the magnetic component, A_t (cm^2)	38.22	31.84	29.6
Mean length of the turn, MLT (cm)	8.93	6.52	5.2	Core geometry coefficient, K_g (cm^5)	0.04507	0.04221	0.04718

Table 5. Optimal transformer characteristics.

Transformer characteristics	Test Case I	Test Case II	Test Case III	Transformer characteristics	Test Case I	Test Case II	Test Case III
Current density, J (A/cm^2)	569.74	833.89	1228.7	Primary turns, N_p	10	31	40
Primary winding resistance, R_p (Ω)	0.0948	0.2719	0.2798	Secondary turns, N_s	12	25	41
Secondary winding resistance, R_s (Ω)	0.1138	0.2192	0.2868	Skin depth, γ (cm)	0.0242	0.0662	0.0209
Total copper losses, P_{cu} (W)	3.908	6.388	4.9034	Primary wire area, A_{wp} (cm^2)	0.00516	0.00128	0.00144
Core losses, P_{fe} (W)	0.3757	0.5506	0.8911	Secondary wire area, A_{ws} (cm^2)	0.00596	0.00379	0.00193
Watt density, λ (W/cm^2)	0.112	0.218	0.196	No. of strands, S_n	4	3	2
Regulation, α (%)	1.5	1.25	0.6473	Specific loss, W_{pk} (W/kg)	14.45	25	38.74
Flux density, B_{mnew} (T)	0.1039	0.1081	0.1267	Temperature rise, ΔT (°C)	7.381	12.78	11.7

up table for the core data is created with the details obtained from the leading magnetic component suppliers, Magnetics®. Table 5 presents the electric, magnetic, and geometric characteristics of the transformer calculated from the optimal core data.

It is inferred from Table 5 that the design optimization procedure based on core geometry coefficient proposed in this paper is effective in solving the HF transformer design problem in a simple, yet efficient manner while keeping all the operational parameters like % regulation, temperature rise and system losses within desired limits. Though all the algorithms used for solving the proposed design problem produce the same optimal values for the parameters under consideration, a comparative analysis shows that they differ with respect to speed of convergence, consistency in producing solutions in successive runs, and the speed of computation.

Figure 5 shows the convergence of the optimization algorithms plotted for Test Case II. This comparison is based on identical population size and equal number of search agents for all the algorithms except GA. As can be seen from the plot, WOA has high speed of convergence followed by PSO, DA, and ALO. However, referring to Figure 6(a), it is clear that among the nature-inspired algorithms, DA is more consistent in producing the optimal results in successive runs. Another interesting fact to be noted is that though WOA is quick to converge compared to PSO algorithm, the relative computational time is the least with PSO (less than a couple of seconds) as portrayed in Figure 6(b). This is because the computational time per iteration is the least with the PSO algorithm.

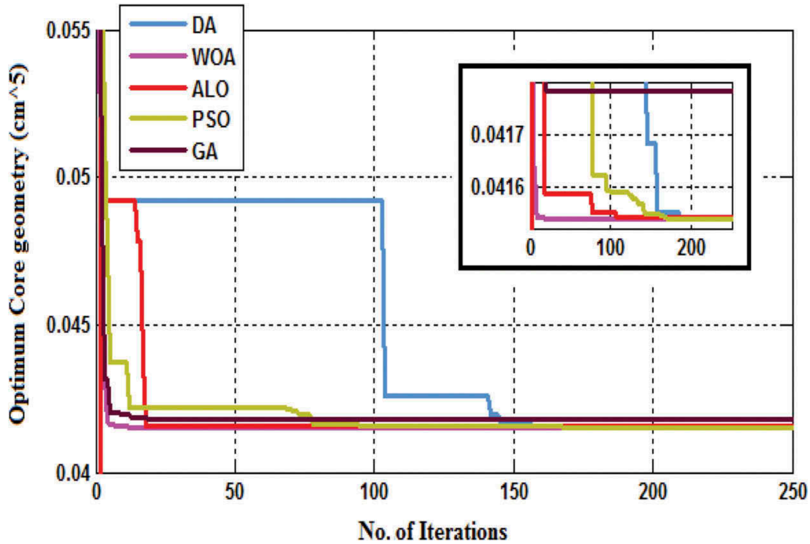

Figure 5. Convergence plot of the optimization algorithms.

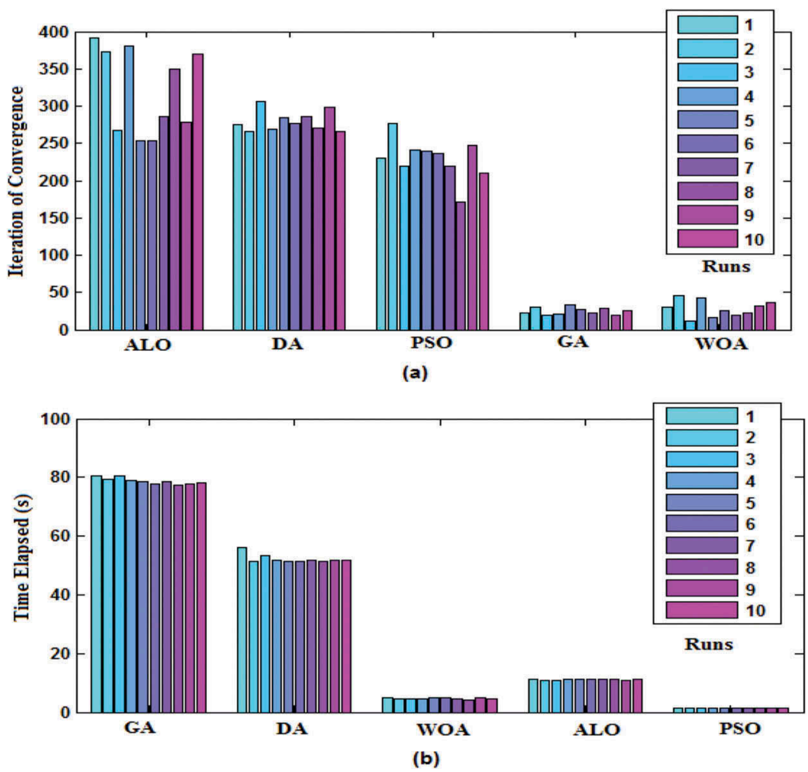

Figure 6. (a) Convergence plot in successive runs. (b) Time plot of convergence in successive runs.

Design validation and results

The proposed design optimization for HF transformers has been tested using PowerEsim, a web-based result-oriented design tool for power converters and transformers (Poon 2009). Unlike traditional tools, PowerEsim is developed using real-world power supplies and components with due consideration to industrial demands and regulations. As such, it is not a simulation tool but a testing tool used by design engineers and trainees from leading industries across the world to verify and improvise their design.

The design validation of the proposed optimization procedure is carried out for one of the test cases (Test Case II) by selecting a half-bridge converter from the available database in PowerEsim. The implemented schematic and the power circuit component specifications are shown in Figure 7 and Table 6, respectively. The Mean Time Between Failure (MTBF) analysis for the overall converter circuit is displayed in Table 7 and that for the HF transformer is depicted in Table 8. The switching waveforms and performance charts presented in Figure 8 reveal the efficiency of the circuit and regulation to be 92.79% and 0.5%, respectively. Figure 9 presents the winding arrangement of the HF transformer. From Figure 10, it can be seen that the choice of

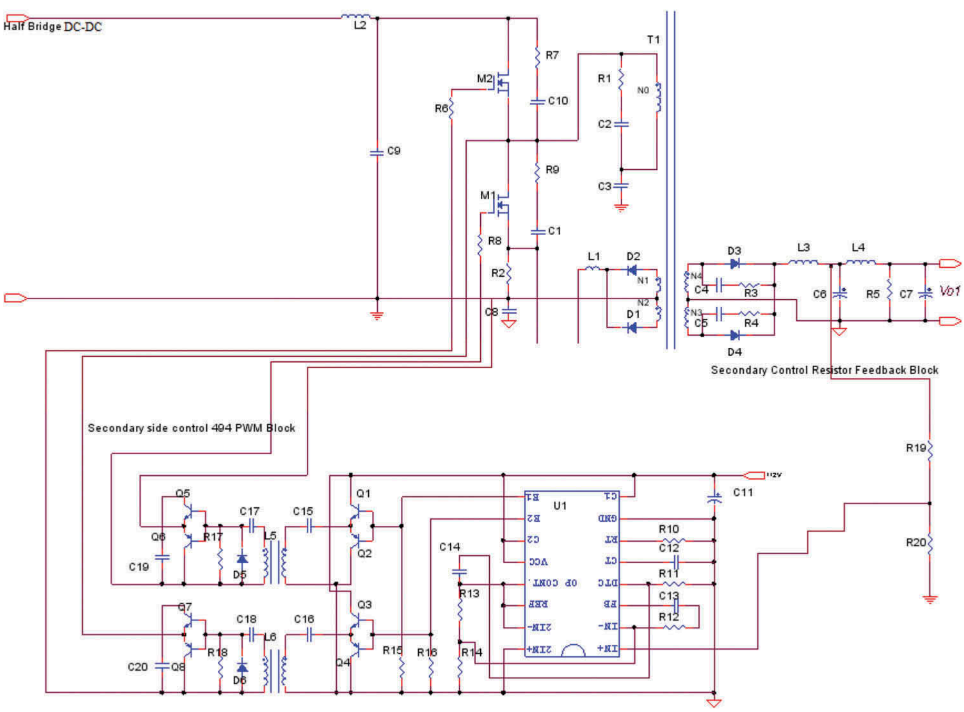

Figure 7. Schematic of the half-bridge DC–DC converter implemented in PowerEsim.

Table 6. Specifications of power circuit components.

T1	177 uH DS-43019-UG P MAGNETICS
M1, M2	0.34 Ohm 600 V 10.6 A
D1, D2	2 A 1.2 kV
D3, D4	12 A 650 V
L1	1.53 mH EE10.5/8/4 Low power switching Inductor
L2	27.8 uH T44-52D Input Differential Mode Choke
L3	229 uH EE42/42/20 Power switching Inductor
L4	10.7 uH T44-52C 52 Noise Filter Choke
C1, C2	100 pF 1 kVdc Y5V 125 Deg. 6.4 × 6.4 × 4 mm Ceramic 5%
C3	3.3 uF 630 Vdc MC 100 Deg. 41.5 × 39.5 × 20 mm PECMPE 20%
C4, C5	510 pF 1.5 kVdc COG 125 Deg. 1.6 × 1.6 × 3.2 mm C1206
C6	220 uF 100 Vdc EC 70 mOhm 105 Deg. 5000 hrs 16 × 25 mm
C7	56 uF 400 Vdc EC 0.795 Ohm 105 Deg. 5000 hrs 22 × 26 mm
C8	4.7 nF 300 Vac Y5V 85 Deg. 18 × 18 × 10 mm
C9	1.5 uF 630 Vdc MC 100 Deg. 31.5 × 26 × 15 mm
C10	100 pF 1 kVdc Y5V 125 Deg. 6.4 × 6.4 × 4 mm Ceramic 5%

Table 7. MTBF analysis of the overall circuit.

At 25 Deg., Standard = MIL-HDBK-217 F
Simulated Overall Failure Rate = 6.264 failures/10^6 hours
Simulated Overall MTBF = 159.6 k hours
Simulated Overall Life Time = 76.08 k hours

Table 8. MTBF analysis of the HF Transformer.

T1	177 uH DS-43019-UG P MAGNETICS transformer_final	Failure Rate = 0.1562 (/10^6 Hrs)
	(1) Bm = 0.121 T	
	(2) Tj = 100 Deg.	
	(3) Wire's Class = 155 Deg. (F)	
	(4) Tape's Class = 130 Deg. (B)	
	(5) Bobbin's Class = 130 Deg. (B)	
	(6) Varnish's Class = 180 Deg. (H)	
	(7) P-S Creepage = Pass	
	(8) Wire Crossed = Pass	

core by PowerEsim tool is a double slab ferrite core with part no. DS43019, similar to the one chosen by the optimization algorithms. However, for the same test case, the choice of the core is HF-5835 with a circuit efficiency as low as 78% using analytical method. This serves as a valid proof for the success of the proposed design optimization procedure for HF transformers in Modular SST applications where regulation and efficiency are considered vital parameters in the design.

Conclusion

This paper has attempted to present a simple, single-objective design optimization procedure for HF transformers used in modular SST applications. The objective was to optimize the core geometry coefficient with a constraint placed on specific loss such that the design produces a

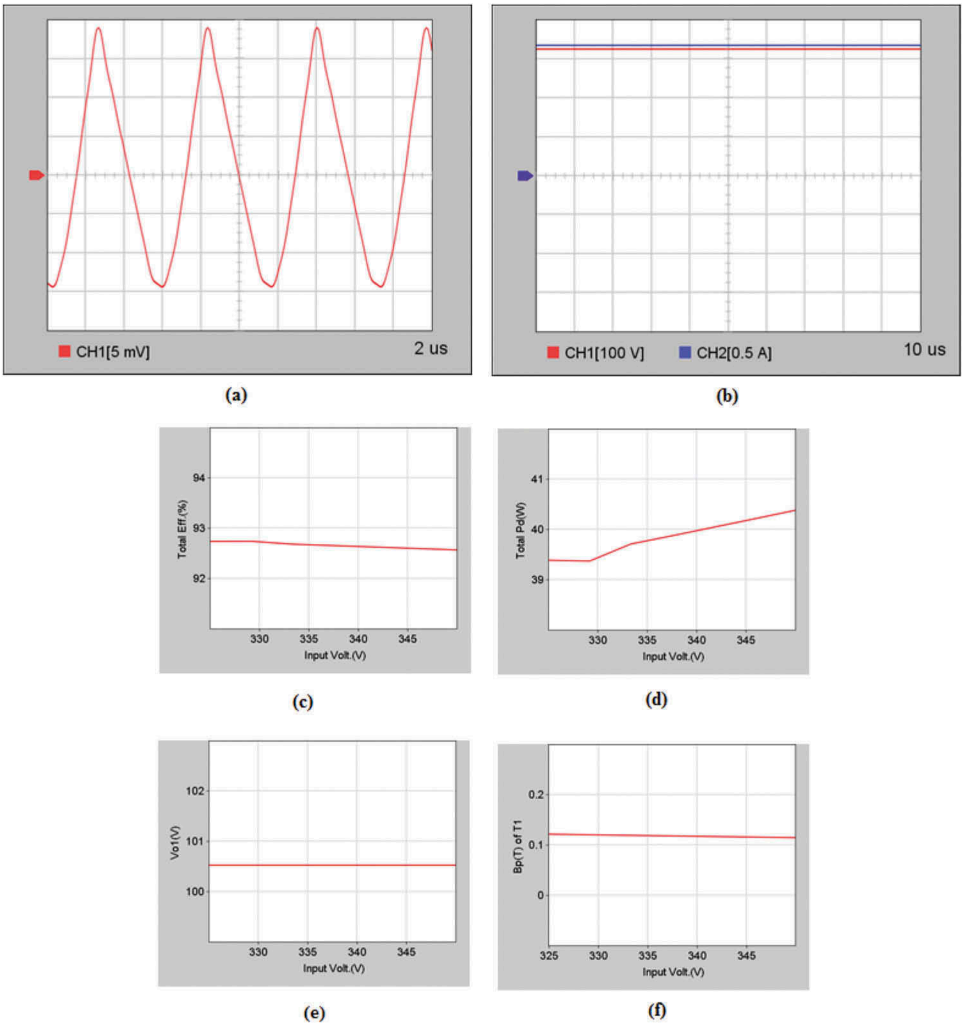

Figure 8. (a) Output switching ripple voltage waveform. (b) Input voltage (CH1) and input current (CH2) waveforms. (c) %Efficiency vs. input voltage. (d) Total dissipated losses vs. input voltage. (e) Output voltage regulation. (f) Variation of peak flux density of the transformer with respect to input voltage.

compact and efficient HF transformer with all performance parameters under preferred limits. Four latest nature-inspired algorithms were engaged to accomplish the proposed optimization task and the results compared with GA. It was found that WOA exhibited quick convergence whereas PSO offered best overall performance with respect to convergence and computational time. The proposed optimization procedure was implemented using PowerEsim, a real-time design tool as well and the results were found to be satisfactory.

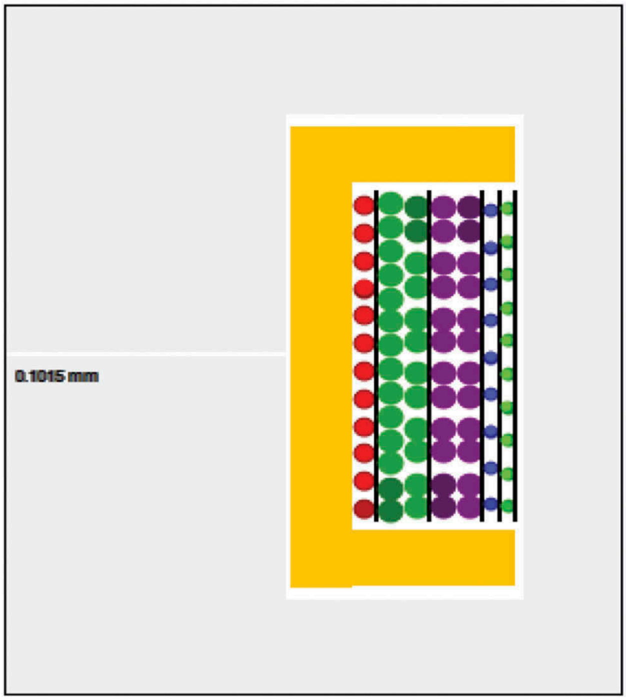

Figure 9. Winding arrangement of HF transformer.

The highlights of the research work are listed below

- This paper is a maiden attempt to optimize the HF transformer based on core geometry (in 5th power of cm) with a constraint imposed on its specific loss keeping regulation and temperature rise within limits in addition to preserving desired efficiency.
- Further, the proposed optimization procedure avoids the need for verification of bounds for parameter values as the optimal value established for core geometry directly brings all the operating parameters within desired limits without compromising on efficiency. Additionally, in contrast to other methods where attention need to be paid to avoid saturation effects on magnetic components, the proposed optimization does not have this issue as the core selection is made only after obtaining the optimal core geometry.
- Three recently developed optimization algorithms namely, Whale Optimization algorithm (WOA), Dragonfly Algorithm (DA), and Ant Lion Optimizer (ALO), which have not been applied to transformer design so far are compared with GA and PSO for their efficacy in solving the optimization problem with respect to various parameters.
- Finally, the optimization results are validated through PowerEsim, a web-based testing platform with huge database of real-time components from leading manufacturers across the globe.

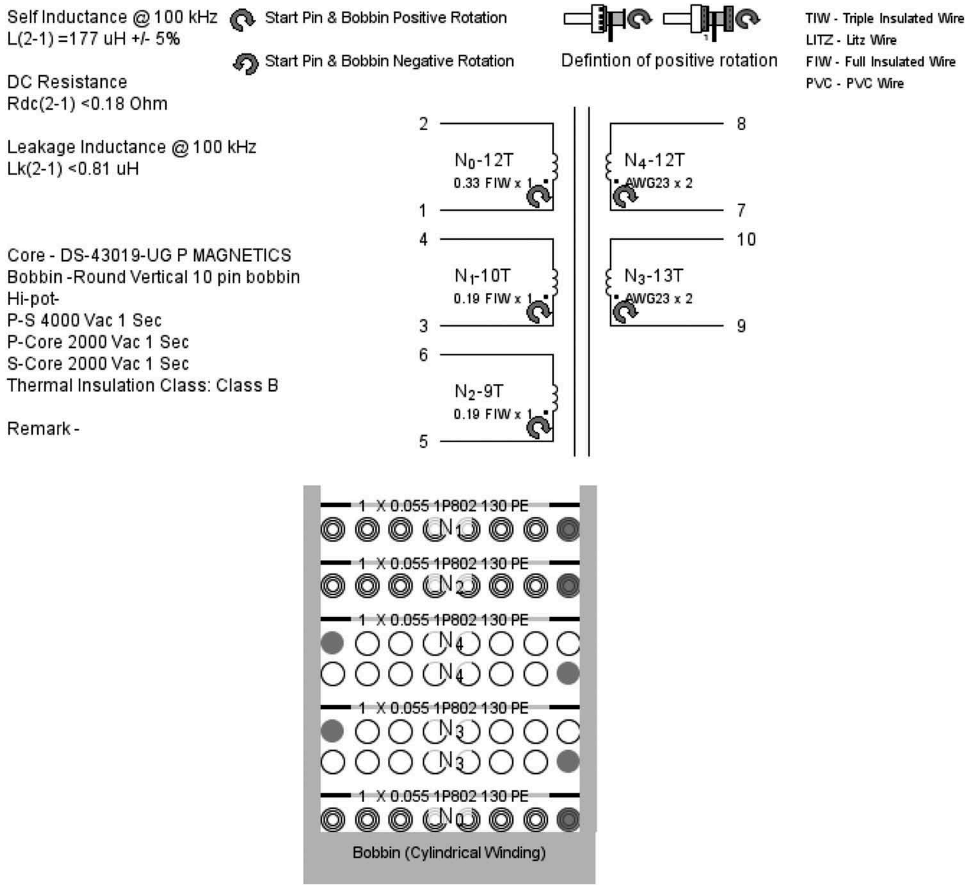

Figure 10. HF transformer design with PowerEsim.

ORCID

Jeyapradha Ravichandran Banumathy http://orcid.org/0000-0001-7432-2860

References

Bahmani, M. A. 2014. *Design and optimization of hf transformers for high power DC-DC applications*. Goteborg, Sweden: Chalmers Reproservice.

Bahmani, M. A., T. Thiringer, and M. Kharezy. 2015. Design methodology and optimization of a medium frequency transformer for high power DC-DC applications. Applied Power Electronics Conference and Exposition (APEC), IEEE, Charlotte, NC, USA, pp. 2532–39.

Breslin, J. G. 2002. Optimisation of high frequency transformer design with arbitrary current and voltage waveforms. PhD. diss., National University of Ireland, Galway. doi:10.1044/1059-0889(2002/er01).

Coonrod, N. R. 1986. Transformer computer design aid for higher frequency switching power supplies. *IEEE Transactions on Power Electronics* 1 (4):248–56. doi:10.1109/TPEL.1986.4766317.

Davood, A., B. Mehdi, and F. Jawad. 2016. Design optimization of cast-resin transformer using nature-inspired algorithms. *Arabian Journal for Science and Engineering* 41 (9): 3491–500.

Du, Y., B. Seunghun, B. Subhashish, and A. Q. Huang. 2010. High-voltage high-frequency transformer design for a 7.2kV to 120V/240V 20kVA Solid State Transformer. Paper presented at the 36th Annual Conference on IEEE Industrial Electronics Society (IECON), Glendale, AZ, USA.

Farhangi, S., and A. Akmal. 1999. A simple and efficient optimization routine for design of high frequency power transformers. Paper presented at the 9th EPE Conference, Graz, Austria.

Hoang, K. D., and J. Wang. 2012. Design optimization of high frequency transformer for dual active bridge DC-DC converter. Paper presented at the XXth International Conference on Electrical Machines, IEEE, Marseille, France, pp.2311–17.

Huina, Y., W. Xiaodong, and W. Gang. 2012. Design of electronic transformer used in a proposed circuit topology for PET. Paper presented at the Power and Energy Engineering Conference (APPEEC), IEEE, Shangai, China, pp.1–4.

Hurley, W. G., W. H. Wolfle, and J. G. Breslin. 1998. Optimized transformer design: Inclusive of high-frequency effects. *IEEE Transactions on Power Electronics* 13 (4):651–59. doi:10.1109/63.704133.

Kjellqvist, T., S. Norrga, and S. Ostlund. 2004. Design considerations for a medium frequency transformer in a line side power conversion system. Paper presented at the 35th Annual IEEE Power Electronics Specialists Conference, IEEE, Aachen, Germany.

Kolar, J. W., and G. Ortiz. 2014. Solid-state-transformers: Key components of future traction and smart grid systems. Proceedings of the International Power Electronics Conference-ECCE Asia (IPEC), pp. 18–21.

McLyman Colonel, W. T. 1993. *Designing magnetic components for high frequency DC-DC converters*. USA: Kg Magnetics Inc.

Meier, S., T. Kjellqvist, S. Norrga, and H. P. Nee. 2009. Design considerations for medium-frequency power transformers in offshore wind farms. *IEEE 13th European Conference on Power electronics and applications EPE*, Barcelona, Spain. 1–12.

Mirjalili, S. 2015. The Ant Lion Optimizer. *Advances in Engineering Software, Elsevier Publishers* 83:80–98. doi:10.1016/j.advengsoft.2015.01.010.

Mirjalili, S. 2016a. The whale optimization algorithm. *Advances in Engineering Software, Elsevier Publishers* 95:51–67. doi:10.1016/j.advengsoft.2016.01.008.

Mirjalili, S. 2016b. Dragonfly algorithm: A new meta-heuristic optimization technique for solving single- objective, discrete, and multi-objective problems. *Neural Computing and Applications* 27 (4):1053–73. doi:10.1007/s00521-015-1920-1.

Montoya, R. J. G., A. Mallela, and J. C. Balda. 2015. An evaluation of selected solid-state transformer topologies for electric distribution systems. Applied Power Electronics Conference and Exposition (APEC), IEEE, Charlotte, NC, USA, pp. 1022–29.

Ortiz, G., J. Biela, and J. W. Kolar. 2010. Optimized design of medium frequency transformers with high isolation requirements. Paper presented at the 36th Annual Conference on IEEE Industrial Electronics Society (IECON), Glendale, AZ, USA.

Ortiz, G., M. Leibl, J. W. Kolar, and O. Apeldoorn. 2013. Medium frequency transformers for solid-state-transformer applications - design and experimental verification. Paper presented at the 10th IEEE International Conference on Power Electronics and Drive Systems (PEDS), Kitakyushu, pp. 1285–90.

Peng, S., and B. Jurgen. 2013. Design and optimization of medium frequency, medium voltage transformers. Paper presented at the 15th European Conference on Power Electronics and Applications (EPE), IEEE, Lille, France, pp.1–10.

Petkov, R. 1996. Optimum design of a High-Power, High-Frequency transformer. *IEEE Transactions on Power Electronics* 11 (1):33–42. doi:10.1109/63.484414.

Poon, N. K. 2009. PowerEsim-free on-line result oriented design tool. Paper presented at the 3rd International Conference on Power Electronics Systems and Applications, IEEE, Hong Kong, China.

Pressman, A. I. 1998. *Switching power supply design*. *2nd* ed., McGraw-Hill, *USA*.

Rama Rao, K. S., Y. L. Lai, T. Soib., and S. Masri. 2004. Design optimization of a high frequency power transformer for a switching power supply by genetic algorithms approach. *Open access repository of USM Research and Publication*.

She, X., Y. Xunwei, W. Fei, and A. Q. Huang. 2014. Design and demonstration of a 3.6-kV–120-V/10-kVA solid-state transformer for smart grid application. *IEEE Transactions on Power Electronics* 29 (8):3982–96. doi:10.1109/TPEL.2013.2293471.

Shri, A. 2013. A solid-state transformer for interconnection between the medium- and the low-voltage grid design. Master of Science Thesis Report, Delft University of Technology, Netherlands.

Steiner, M., and H. Reinold. 2007. Medium frequency topology in railway applications. Paper presented at the European Conference on Power Electronics and Applications, IEEE, Aalborg, Denmark.

Versèle, C., O. Deblecker, and J. Lobry. 2012. A computer-aided design tool dedicated to isolated DC-DC converters based on multiobjective optimization using genetic algorithms. *COMPEL - the International Journal for Computation and Mathematics in Electrical and Electronic Engineering* 31 (2):583–603. doi:10.1108/03321641211200590.

Vinnikov, D., T. Jalakas, and M. Egorov. 2008. Feasibility study of half- and full-bridge isolated DC/DC converters in High-Voltage High-Power applications. Paper presented at the 13thPower Electronics and Motion Control Conference, EPE-PEMC, Poznan, Poland.

Yadav, A. K., O. P. Rahi, H. Malik, and A. Azeem. 2011. Design optimization of high-frequency power transformer by genetic algorithm and simulated annealing. *International Journal of Electrical and Computer Engineering (IJECE)* 1 (2):102–09. doi:10.11591/ijece.v1i2.88.

Yang, X.-S. 2010. *Nature-inspired meta heuristic algorithms*. 2nd ed. UK: Luniver Press.

Appendix

(1) Maximum Duty ratio, $D_{\max} = \frac{1}{T}\left(\frac{T}{2} - t_{dw}\right)$

where T is the total time period and t_{dw} is the dwell time (1 μs)

(2) Secondary load power for single winding in Watts, $P_{ts} = I_o(V_o + V_d)$

Secondary load power for tapped winding in Watts, $P_{ts} = I_o(V_o + V_d) * \sqrt{2}$

(3) Total Apparent Power in Watts, $P_t = P_{ts}(1 + \frac{1}{\eta})$

(4) Average primary current in amps, $I_{pri} = \frac{2P_{ts}}{V_{in} * \eta}$ (for half-bridge converter)

(5) Average primary voltage in Volts, $V_{pri} = \frac{V_{in}}{2}(2D_{\max}) - I_{pri}R_q$

where R_q is the on resistance of transistor in Ohms

(6) Primary turns, $N_p = \frac{V_{pri} \times 10^4}{K_f B_{m\_opt} f_{opt} A_c}$

(7) Current density in amps/cm^2, $J = \frac{P_t \times 10^4}{K_f K_u B_{m\_opt} f_{opt} A_p}$

(8) Primary rms current in amps, $I_{prms} = \frac{I_{pri}}{\sqrt{2D_{\max}}}$

(9) Primary wire area in cm^2, $A_{wp} = \frac{I_{prms}}{J}$

(10) Skin Depth in cm, $\gamma = \frac{6.62}{\sqrt{f_{opt}}}$

(11) Wire area in cm^2, $A_{wire} = \pi\gamma^2$
(12) Primary winding resistance in Ohms, $R_p = MLT\left(N_p\right)\left(\frac{\mu\Omega}{cm}\right) \times 10^{-6}$
(13) Primary copper loss in Watts, $P_{pcu} = {I_{prms}}^2 R_p$
(14) Secondary turns on each side of center tap, $N_s = \frac{N_p(V_o+V_d)}{V_{pri}}$
(15) Secondary wire area in cm^2, $A_{ws} = \frac{I_o\sqrt{D_{\max}}}{J}$
(16) No. of strands required, $S_n = \frac{A_{ws}}{A_{wire}(b)}$, where A_{wire} *(b)* is the bare wire area from the wire table
(17) Secondary winding resistance in ohms, $R_s = MLT(N_p)\frac{\mu\Omega}{cm}X10^{-6}$
(18) Secondary copper loss in Watts, $P_{scu} = {I_o}^2 R_s$
(19) Total copper loss in Watts, $P_{cu} = P_{pcu} + P_{scu}$
(20) Window utilization factor, $K_{unew} = \frac{N_p S_n A_{wire}(b) + N_s S_n A_{wire}(b)}{W_a}$
(21) Regulation in %, $\alpha_{new} = \frac{P_{cu}}{P_o}X100$
(22) Flux Density in Tesla, $B_{mnew} = \frac{V_{pri}X10^4}{K_f f_{opt} A_c N_p}$
(23) Watts per kilogram, $WK = 3.18X10^{-4}(f_{opt})^{1.51}(B_{mnew})^{2.747}$
(24) Core loss in Watts, $P_{fe} = WK(W_{tfe})X10^{-3}$
(25) Total Losses in Watts, $P_{tot} = P_{cu} + P_{fe}$
(26) Watt density in Watts/cm^2, $\lambda = \frac{P_{tot}}{A_t}$

Temperature rise in ℃, $\Delta T = 450(\lambda)^{0.826}$